2.42-2.49 (1 H, m), 2.52 (3 H, s), 2.90 (3 H, s), 2.99-3.02 (1 H, m), 3.16-3.18 (1 H, m), 3.33-3.36 (1 H, m), 3.54-3.59 (2 H, m), 3.69 (1 H, m), 3.78 (3 H, s), 3.98-4.01 (2 H, m), 4.14-4.20 (1 H, m), 4.54-4.57 (2 H, m), 4.76-4.82 (2 H, m), 5.03-5.09 (1 H, m), 5.10-5.13 (1 H, m), 5.16-5.17 (1 H, d, J = 3.6 Hz), 6.82 (2 H, d, J = 8.4 Hz), 7.0 (1 H, m), 7.05 (2 H, d, J = 8.5 Hz), 7.33 (1 H, m, J = 8.5 Hz), 7.87 (1 H, m); HRMS calcd for $C_{52}H_{83}N_6O_{14}$ (M + H) 1015.5967, found 1015.5831.

Acknowledgment. Support from NIH (CA-40081) and a small instrumentation grant from the University of Pennsylvania Research Foundation is gratefully acknowledged. We thank Professor C. Francisco from the University of Perpignan for the gift of a didemnin B sample, the group of Professor B. Castro at the CNRS-INSERM, Montpellier, for sharing information with us, and Drs. G. Furst, J. Dykins, and P. Carroll of the University of Pennsylvania Spectroscopic Facilities for their expert technical assistance.

Syntheses of Macrocyclic Enzyme Models. 7.† Octopus Cyclophanes Having L-Aspartate Residues as Novel Water-Soluble Hosts. Aggregation Behavior and Induced-Fit Molecular Recognition

Yukito Murakami,* Jun-ichi Kikuchi,‡ Teruhisa Ohno, Osamu Hayashida, and Masayo Kojima

Contribution No. 922 from the Department of Organic Synthesis, Faculty of Engineering, Kyushu University, Fukuoka 812, Japan. *Received March 29, 1990*

Abstract: Octopus cyclophanes (**1** and **2**), having chiral L-aspartate residues as connector units interposed between a rigid 2,11,20,29-tetraaza[3.3.3.3]paracyclophane skeleton and four double-chain hydrocarbon segments, were prepared. Aggregation behavior of the octopus cyclophanes in aqueous media was characterized by means of electron microscopy as well as by surface tension and dynamic light scattering measurements. Its consequence in guest recognition was clarified by employing ^{1}H NMR, fluorescence, and circular dichroism (CD) spectroscopy. Multiwalled bilayer vesicles were observed in an aqueous dispersion of **1** by negative-staining electron microscopy. The present cationic hosts strongly bind anionic and nonionic hydrophobic guests, such as 8-anilinonaphthalene-1-sulfonate, 6-*p*-toluidinonaphthalene-2-sulfonate, *N*-phenyl-1-naphthylamine, and *N*-phenyl-2-naphthylamine, to form inclusion complexes in 1:1 stoichiometry, regardless of aggregation status of the hosts, monomeric or vesicular. Two types of guest-binding behavior were exercised by the octopus cyclophanes, depending on the nature of media used for preparation of their stock solutions. When an aqueous stock solution of the host was injected into an aqueous buffer containing a guest, the host–guest complexation immediately reached an equilibrium state, as monitored by fluorescence spectroscopy. Concurrently, the chiral L-aspartate residues of the host molecule underwent conformational changes so as to attain effective guest incorporation. ^{1}H NMR spectroscopy applied to the host–guest complexation indicated that the guest molecule was undoubtedly incorporated into the three-dimensional cavity provided intramolecularly by the macrocyclic ring and the eight hydrocarbon chains. On the other hand, when an organic stock solution of **1** in methanol, ethanol, tetrahydrofuran, or dioxane was injected into an aqueous buffer containing a guest, time-dependent and biphasic complexation behavior was observed as reflected in various fluorescence parameters, such as fluorescence intensity, maximum, polarization, lifetime, and rotational correlation time, attributable to the incorporated guest molecule. This behavior is consistent with fast incorporation of a guest molecule into the hydrophobic host cavity followed by slow and long-range conformational changes of the host, as induced by the incorporated guest. Such biphasic complexation behavior was very sensitive to molecular architecture at the connector portions in the hosts. Dynamic aspects of the induced-fit molecular recognition by the present octopus cyclophanes are discussed.

Introduction

The hydrophobic interaction is the prevailing driving force for molecular recognition in aqueous media, and other recognition forces for distinct molecular discrimination, such as electrostatic, hydrogen-bonding, and charge-transfer interactions, become effective in the sufficiently desolvated and hydrophobic microenvironments which are well shielded from bulk aqueous phase. As artificial hosts capable of providing hydrophobic recognition sites, macrocyclic compounds bearing sizable internal cavities, such as cyclophanes[1-4] and cyclodextrins,[5,6] and molecular aggregates composed of amphiphiles,[7] such as micelles and bilayer membranes, have been widely employed. While macrocyclic hosts primarily perform the lock-and-key-type discrimination toward guest molecules due to their geometrically restricted hydrophobic cavities provided by rigid frameworks, amphiphiles provide geometrically flexible recognition sites as controlled by their aggregate morphology.

Synthetic approaches to the development of macrocyclic hosts exhibiting induced-fit functions have so far been carried out to a limited extent.[8] We have recently developed novel hosts, so-

† For part 6 of this series, see ref 11.

‡ Present address: Department of Applied Chemistry, Faculty of Science and Engineering, Saga University, Saga 840, Japan.

(1) Tabushi, I.; Yamamura, K. *Top. Curr. Chem.* **1983**, *113*, 145-185.
(2) (a) Murakami, Y. *Top. Curr. Chem.* **1983**, *115*, 107-155. (b) Murakami, Y. *J. Inclusion Phenom.* **1984**, *2*, 35-47. (c) Murakami, Y.; Kikuchi, J. *Pure Appl. Chem.* **1988**, *60*, 549-554.
(3) Odashima, K.; Koga, K. In *Cyclophanes*; Keehn, P. M., Rosenfeld, S. M., Eds.; Academic Press: New York, 1983; Vol. 2, Chapter 11.
(4) Diederich, F. *Angew. Chem., Int. Ed. Engl.* **1988**, *27*, 362-386.
(5) (a) Bender, M. L.; Komiyama, M. *Cyclodextrin Chemistry*; Springer: Berlin, 1978. (b) D'Souza, V. T.; Bender, M. L. *Acc. Chem. Res.* **1987**, *20*, 146-158.
(6) (a) Breslow, R. *Science (Washington, DC)* **1982**, *218*, 532-537. (b) Breslow, R. *Adv. Enzymol. Relat. Areas Mol. Biol.* **1986**, *58*, 1-60.
(7) Fendler, J. H. *Membrane Mimetic Chemistry*; John Wiley: New York, 1982.

0002-7863/90/1512-7672$02.50/0

called octopus cyclophanes, by introduction of multiple amphiphilic components into a rigid macrocyclic skeleton.[8-12] These hosts exhibit the following unique functions with regard to molecular recognition in aqueous media: (1) The host molecules provide cavities that are deep and hydrophobic enough to incorporate hydrophobic guests of various bulkinesses through an induced-fit mechanism originating from the flexible character of the alkyl branches. (2) Electrostatic and charge-transfer interactions in addition to hydrophobic interactions come into play in the host–guest complexation process, so that the binding of guest molecules is enhanced. (3) Formation of both 1:1 and 1:2 host–guest complexes is favored so long as electrostatic repulsion between guest molecules is not operative in the hydrophobic cavity. (4) The hydrophobic cage provided by the octopus cyclophane is highly apolar and acts to suppress the molecular motion of guests. Thus, octopus cyclophanes can be used as apoenzyme models for effective simulation of enzymatic functions.[12-15]

In order to get further insights into the induced-fit binding behavior of octopus cyclophanes toward various guests, we now prepared two octopus cyclophanes each having L-aspartate residues, **1** and **2** (Chart I). The chiral molecular components were introduced as connector units, interposed between a tetraaza[3.3.3.3]paracyclophane skeleton as an octopus body and hydrocarbon branches as hydrophobic arms. In this article, we report on their aggregation behavior and unique guest-binding behavior in aqueous media with emphasis on the first successful observations of dynamic features of induced-fit host–guest complexation.

Experimental Section

Materials. The following compounds were obtained from commercial sources as guaranteed reagents and used without further purification: magnesium bis(8-anilinonaphthalene-1-sulfonate) [$Mg(ANS)_2$], potassium 6-*p*-toluidinonaphthalene-2-sulfonate [K(TNS)], and [[1-(dimethylamino)naphthalene-5-sulfonamido]ethyl]trimethylammonium perchlorate [(DASP)ClO_4] (all from Nacalai Tesque, Inc., Kyoto, Japan). *N*-Phenyl-1-naphthylamine (α-PNA) and *N*-phenyl-2-naphthylamine (β-PNA) (both from Tokyo Kasei Kogyo Co., Tokyo, Japan) were recrystallized from methanol–water (4:1 v/v) (mp 61–62 °C) and methanol–water (5:1 v/v) (mp 108–109 °C), respectively. N^{α}-(*tert*-butoxycarbonyl)-L-asparlic acid β-benzyl ester (**3**) was purchased from Peptide Institute, Inc., Osaka, Japan, as a guaranteed reagent. 2,11,20,29-Tetraaza[3.3.3.3]paracyclophane (**4**) was prepared after a method reported previously[16] [M^+ (EI ionization) 476].

***N*,*N*-Ditetradecyl-N^{α}-(*tert*-butoxycarbonyl)-L-isoasparagine β-Benzyl Ester (5).** Dicyclohexylcarbodiimide (1.8 g, 8.9 mmol) was added to a solution of N^{α}-(*tert*-butoxycarbonyl)-L-aspartic acid β-benzyl ester (**3**) (2.5 g, 8.0 mmol) in dry dichloromethane (17 mL) at 0 °C, and the mixture was allowed to stand at the same temperature while being stirred for 20 min. Ditetradecylamine (3.3 g, 8.0 mmol) in dry dichloromethane (8.5 mL) was added to the mixture, and the resulting mixture was stirred for 4 h at 0 °C and for additional 17 h at room temperature. Precipitates that formed (*N*,*N*′-dicyclohexylurea) were removed by filtration, the solvent was eliminated under reduced pressure, and the residue was dissolved in ethyl acetate (70 mL). The solution was then washed with 10% aqueous citric acid (60 mL × 3), saturated aqueous sodium chloride (60 mL × 3), and 4% aqueous sodium hydrogen carbonate (60 mL × 3) in this sequence. After being dried (Na_2SO_4), the solution was evaporated to dryness under reduced pressure. The residue was chromatographed on a column of silica gel (Wako Gel C-100) with acetone as eluant. The product fraction was dried in vacuo to give a colorless oil (3.2 g, 56%): IR (KBr disc) 2920 and 2860 (CH), and 1710 and 1640 (C=O) cm^{-1}; NMR (400 MHz, $CDCl_3$) δ_H 0.87 [6 H, t, *J* 7.0 Hz, $(CH_2)_{13}CH_3$], 1.23 [48 H, m, $CH_2(CH_2)_{12}CH_3$], 1.38 [9 H, s, $(CH_3)_3CO$], 2.63 [1 H, dd, J_{vic} 7.3 Hz and J_{gem} 15.0 Hz, CH_2COO (nonequivalent)], 2.83 [1 H, dd, J_{vic} 6.5 Hz and J_{gem} 15.0 Hz, CH_2COO (nonequivalent)], 3.2–3.5 [4 H, m, $CH_2(CH_2)_{12}CH_3$], 4.95 [1 H, m,

Chart I

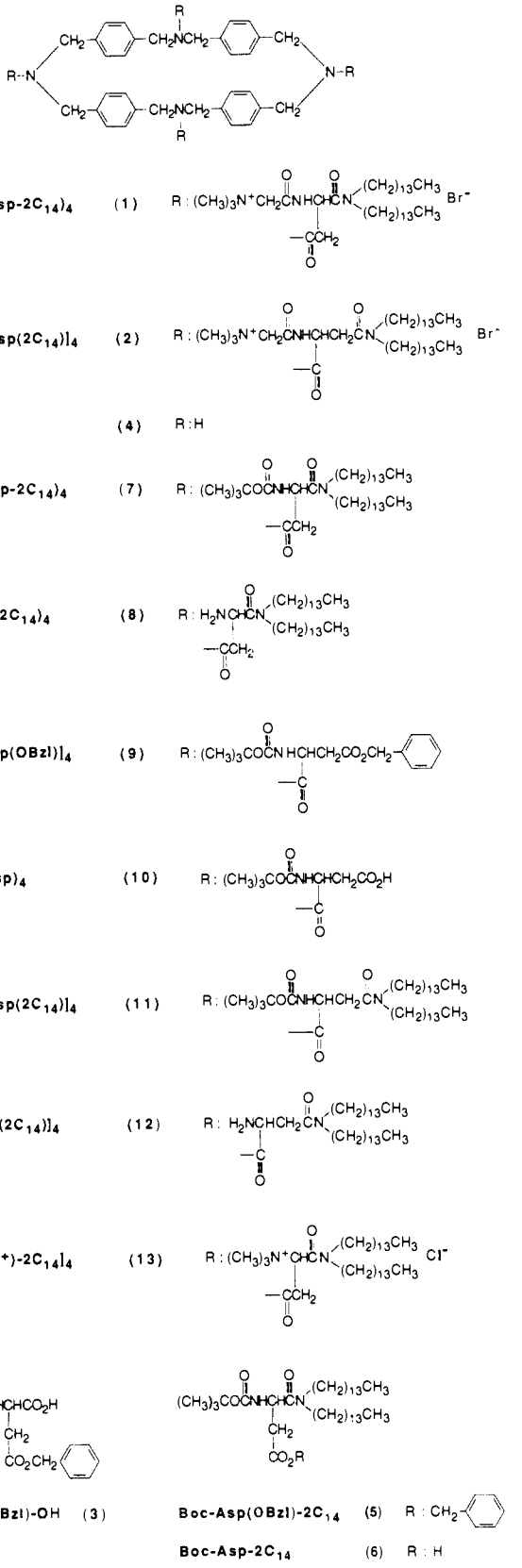

(8) (a) Murakami, Y.; Nakano, A.; Miyata, R.; Matsuda, Y. *J. Chem. Soc., Perkin Trans. 1* **1979**, 1669–1676. (b) Murakami, Y.; Nakano, A.; Akiyoshi, K.; Fukuya, K. *J. Chem. Soc., Perkin Trans. 1* **1981**, 2800–2808. (c) Murakami, Y.; Kikuchi, J.; Tenma, H. *J. Chem. Soc., Chem. Commun.* **1985**, 753–755. (d) Hamilton, A. D.; Van Engen, D. *J. Am. Chem. Soc.* **1987**, *109*, 5035–5036. (e) Schneider, H.-J.; Gütes, D.; Schneider, U. *J. Am. Chem. Soc.* **1988**, *110*, 6449–6454. (f) Menger, F. M.; Takeshita, M.; Chow, J. F. *J. Am. Chem. Soc.* **1981**, *103*, 5938–5939.

(9) Murakami, Y.; Kikuchi, J.; Suzuki, M.; Takaki, T. *Chem. Lett.* **1984**, 2139–2142.

(10) Murakami, Y.; Kikuchi, J.; Tenma, H. *Chem. Lett.* **1985**, 103–106.

(11) Murakami, Y.; Kikuchi, J.; Suzuki, M.; Matsuura, T. *J. Chem. Soc., Perkin Trans. 1* **1988**, 1289–1299.

(12) Murakami, Y.; Kikuchi, J.; Hayashida, O. *J. Inclusion Phenom.* **1989**, *7*, 91–97.

(13) Murakami, Y.; Hisaeda, Y.; Kikuchi, J.; Ohno, T.; Suzuki, M.; Matsuda, Y. *Chem. Lett.* **1986**, 727–730.

(14) Murakami, Y.; Hisaeda, Y.; Kikuchi, J.; Ohno, T.; Suzuki, M.; Matsuda, Y. *Stud. Org. Chem.* **1987**, *31*, 433–438.

(15) Murakami, Y.; Hisaeda, Y.; Kikuchi, J.; Ohno, T.; Suzuki, M.; Matsuda, Y.; Matsuura, T. *J. Chem. Soc., Perkin Trans. 2* **1988**, 1237–1246.

(16) Takemura, H.; Suenaga, M.; Sakai, K.; Kawachi, H.; Shinmyozu, T.; Miyahara, Y.; Inazu, T. *J. Inclusion Phenom.* **1984**, *2*, 207–214.

NHC*H*CO], 5.03 [2 H, s, benzyl], 5.29 [1 H, d, *J* 10.0 Hz, CON*H*CH], and 7.21 [5 H, m, ArH]. Anal. Calcd for $C_{44}H_{78}N_2O_5 \cdot {}^1/_4H_2O$: C, 73.44; H, 11.00; N, 3.89. Found: C, 73.52; H, 10.95; N, 3.96.

***N*,*N*-Ditetradecyl-N^{α}-(*tert*-butoxycarbonyl)-L-isoasparagine (6).** Palladium black (10% Pd, 1.0 g) was added to compound **5** (1.6 g, 2.1 mmol) in tetrahydrofuran (27 mL), and hydrogen gas was introduced into the mixture at room temperature for 22 h along with stirring. The catalyst was removed by filtration, and the solvent was eliminated under reduced pressure. The residue was chromatographed on a column of silica gel (Wako Gel C-100) with ethyl acetate as eluant. The product fraction was dried in vacuo to give a pale yellow oil (1.5 g, quantitative): R_f (Tokyo Kasei Silica Gel f; ethyl acetate) 0.86; IR (KBr disc) 2920 and 2860 (CH), and 1640 (C=O) cm^{-1}; NMR (60 MHz, $CDCl_3$) δ_H 0.87 [6 H, t, *J* 7.0 Hz, $(CH_2)_{13}CH_3$], 1.24 [48 H, m, $CH_2(CH_2)_{12}CH_3$], 1.40 [9 H, s, $(CH_3)_3CO$], 2.64 [2 H, bd, CH_2COO], 3.2–3.5 [4 H, m, $CH_2(CH_2)_{12}CH_3$], 4.91 [1 H, m, NHC*H*CO], and 5.50 [1 H, bs, CON*H*CH]. Anal. Calcd for $C_{37}H_{72}N_2O_5 \cdot {}^1/_2H_2O$: C, 70.13; H, 11.61; N, 4.42. Found: C, 70.17; H, 11.40; N, 4.23.

***N*,*N*′,*N*″,*N*‴-Tetrakis[3-(*N*,*N*-ditetradecylcarbamoyl)-3-[(*tert*-butoxycarbonyl)amino]propanoyl]-2,11,20,29-tetraaza[3.3.3.3]paracyclophane (7).** Dicyclohexylcarbodiimide (141 mg, 0.68 mmol) was added to a solution of compound **6** (394 mg, 0.64 mmol) in dry dichloromethane (4.5 mL) at 0 °C, and the mixture was allowed to stand at the same temperature while being stirred for 20 min. Compound **4** (61 mg, 0.13 mmol) in dry dichloromethane (5 mL) was added to the mixture, and the resulting mixture was stirred for 4 h at 0 °C and for additional 44 h at room temperature. Precipitates that formed (*N*,*N*′-dicyclohexylurea) were removed by filtration, and the solvent was eliminated under reduced pressure. The crude product was purified by gel filtration chromatography on a column of Sephadex LH-20 with methanol–chloroform (1:1 v/v) as eluant. Evaporation of the product fraction under reduced pressure gave a colorless solid (240 mg, 64%): mp 65–68 °C; R_f (Wako Silica Gel 70FM; methanol–ethyl acetate (1:1 v/v)) 0.76; IR (KBr disc) 2920 and 2860 (CH), and 1720 and 1640 (C=O) cm^{-1}; NMR (400 MHz, $CDCl_3$) δ_H 0.88 [24 H, t, *J* 7.0 Hz, $(CH_2)_{13}CH_3$], 1.26 [192 H, m, $CH_2(CH_2)_{12}CH_3$], 1.42 [36 H, s, $(CH_3)_3CO$], 2.64 [8 H, bd, $COCH_2CH$], 3.25 [16 H, m, $CH_2(CH_2)_{12}CH_3$], 4.20–4.55 [16 H, bs, CH_2Ph], 5.05–5.20 [8 H, m, NHC*H*CO and CON*H*CH], and 6.84 [16 H, m, ArH]. Anal. Calcd for $C_{180}H_{316}N_{12}O_{16} \cdot 2H_2O$: C, 73.52; H, 10.83; N, 5.72. Found: C, 73.53; H, 10.75; N, 5.88.

***N*,*N*′,*N*″,*N*‴-Tetrakis[3-(*N*,*N*-ditetradecylcarbamoyl)-3-aminopropanoyl]-2,11,20,29-tetraaza[3.3.3.3]paracyclophane (8).** Trifluoroacetic acid (7 mL) was added to a solution of compound **7** (190 mg, 6.5 × 10^{-5} mol) in dry dichloromethane (20 mL), and the mixture was stirred for 2 h at room temperature. After the solvent was evaporated off under reduced pressure, the crude product was purified by gel filtration chromatography on a column of Sephadex LH-20 with methanol as eluant. Evaporation of the solvent under reduced pressure gave a colorless glassy solid (150 mg, 93%): IR (KBr disc) 2920 and 2860 (CH), and 1650 (C=O) cm^{-1}; NMR (60 MHz, $CDCl_3$) δ_H 0.85 [24 H, t, *J* 7.0 Hz, $(CH_2)_{13}CH_3$], 1.24 [192 H, m, $CH_2(CH_2)_{12}CH_3$], 2.70 [8 H, m, $COCH_2CH$], 3.30 [16 H, m, $CH_2(CH_2)_{12}CH_3$], 4.37 [20 H, m, CH_2Ph and $COCH_2CH$], and 6.80 [16 H, m, ArH]. Anal. Calcd for $C_{160}H_{284}N_{12}O_8 \cdot 2H_2O$: C, 75.66; H, 11.43; N, 6.62. Found: C, 75.81; H, 11.21; N, 6.89.

***N*,*N*′,*N*″,*N*‴-Tetrakis[3-*N*,*N*-ditetradecylcarbamoyl)-3-[(trimethylammonio)acetamido]propanoyl]-2,11,20,29-tetraaza[3.3.3.3]paracyclophane Tetrabromide (1).** Triethylamine (0.2 mL, 2.4 mmol) and compound **8** (150 mg, 6.0 × 10^{-5} mol) were dissolved in dry dichloromethane (5 mL), and the solution was cooled to 0 °C. Bromoacetyl chloride (0.13 g, 0.77 mmol) in dry dichloromethane (5 mL) was added dropwise to the solution at 0 °C with stirring, and the mixture was stirred for 2 h at 0 °C and for additional 18 h at room temperature. The resulting mixture was evaporated to dryness under reduced pressure. The residue was dissolved in dichloromethane (30 mL) and washed with 4% aqueous sodium hydrogen carbonate (25 mL × 1), 4% aqueous citric acid (25 mL × 1), and saturated aqueous sodium chloride (25 mL × 1) in this sequence. After being dried (Na_2SO_4), the solution was evaporated to dryness under reduced pressure, and the residue was dissolved in tetrahydrofuran (25 mL). Dry trimethylamine gas was introduced into this solution for 3 h at room temperature, and the solution was stirred at the same temperature for 48 h. The solvent was evaporated off under reduced pressure, and the crude product was purified by gel filtration chromatography on a column of Sephadex LH-20 with methanol as eluant. Evaporation of the solvent under reduced pressure gave a pale yellow solid (100 mg, 51.7%): mp 136–138 °C; IR (KBr disc) 2920 and 2860 (CH), and 1686 and 1646 (C=O) cm^{-1}; NMR (400 MHz, $CDCl_3$) δ_H 0.89 [24 H, t, *J* 7.0 Hz, $(CH_2)_{13}CH_3$], 1.28 [192 H, m, $CH_2(CH_2)_{12}CH_3$], 2.90 [8 H, bd, $COCH_2CH$], 3.30–3.50 [16 H, m, $CH_2(CH_2)_{12}CH_3$], 3.30 [36 H, s, $N^+(CH_3)_3$], 4.12 [8 H, m, $COCH_2N^+(CH_3)_3$], 4.20–4.70 [16 H, m, CH_2Ph], 5.35 [8 H, m, CON*H*CH and CONHC*H*], and 6.93–7.00 [16 H, bd, ArH]; δ_C (100 MHz, CD_3OD) 15.4 [$(CH_2)_{13}CH_3$], 24.6 [$(CH_2)_{12}CH_2CH_3$], 28.7 [$(CH_2)_2CH_2(CH_2)_{10}CH_3$], 28.8 [$COCH_2CH$], 29.4 [$(CH_2)_{10}CH_2(CH_2)_2CH_3$], 30.9 [$(CH_2)_3(CH_2)_7(CH_2)_3CH_3$], 31.7 [$(CH_2)_{11}CH_2CH_2CH_3$], 33.9 [$CH_2CH_2(CH_2)_{11}CH_3$], 49.7 [$NCH_2(CH_2)_{12}CH_3$], 50.0 [$CH_2CHNH$], 50.2 [$N^+(CH_3)_3$], 50.4 [$CH_2Ph$], 55.7 [$COCH_2N^+(CH_3)_3$], 129.5 (C-5, -6, -8, -9, -14, -15, -17, -18, -23, -24, -26, -27, -32, -33, -35, and -36), 138.5 (C-4, -7, -13, -16, -22, -25, -31, and -34), 164.9 [$COCH_2N^+(CH_3)_3$], and 172.5 [CH_2CON and CH_2CHCON]. Anal. Calcd for $C_{180}H_{324}Br_4N_{16}O_{12} \cdot 2H_2O$: C, 66.31; H, 10.14; N, 6.87. Found: C, 66.35; H, 9.90; N, 6.85.

***N*,*N*′,*N*″,*N*‴-Tetrakis[3-(*N*,*N*-ditetradecylcarbamoyl)-3-(trimethylammonio)propanoyl]-2,11,20,29-tetraaza[3.3.3.3]paracyclophane Tetrachloride (13).** Methyl iodide (15 mL) and sodium hydrogen carbonate (435 mg, 4.0 × 10^{-3} mol) was added to compound **8** (100 mg, 4.0 × 10^{-5} mol) dissolved in dry dimethylformamide (12 mL). The mixture was deoxygenated by the freeze–pump–thaw method and stirred for 70 h at 90 °C. After precipitates were removed from the mixture by filtration, the filtrate was evaporated to dryness under reduced pressure. The residue was dissolved in chloroform (10 mL) and evaporated to dryness under reduced pressure after an insoluble material was removed by filtration. The resulting iodide salt was converted into the chloride salt by ion-exchange chromatography on a column of Amberlite IRA-401 with methanol as eluant. The solvent was evaporated off under reduced pressure, and the crude product was purified by gel filtration chromatography on columns of Sephadex LH-20 and Toyopearl HW-40F with methanol as eluant. Evaporation of the solvent under reduced pressure gave a colorless solid (58 mg, 51.7%): mp 142–144 °C; IR (KBr disc) 1650 (C=O) cm^{-1}; NMR (400 MHz, $CDCl_3$) δ_H 0.89 [24 H, t, *J* 7.0 Hz, $(CH_2)_{13}CH_3$], 1.28 [192 H, m, $CH_2(CH_2)_{12}CH_3$], 3.30 [36 H, s, $N^+(CH_3)_3$], 3.40 [8 H, bd, $COCH_2CH$], 3.30–3.50 [16 H, m, $CH_2(CH_2)_{12}CH_3$], 4.20–4.70 [16 H, m, CH_2Ph], 5.15 [4 H, m, CONHC*H*], and 6.93–7.00 [16 H, bd, ArH]; δ_C (100 MHz, CD_3OD) 14.6 [$(CH_2)_{13}CH_3$], 23.8 [$(CH_2)_{12}CH_2CH_3$], 28.1 [$(CH_2)_2CH_2(CH_2)_{10}CH_3$], 28.2 [$COCH_2CH$], 29.5 [$(CH_2)_{10}CH_2(CH_2)_2CH_3$], 30.5 [$(CH_2)_3(CH_2)_7(CH_2)_3CH_3$], 31.4 [$(CH_2)_{11}CH_2CH_2CH_3$], 33.1 [$CH_2CH_2(CH_2)_{11}CH_3$], 49.2 [$NCH_2(CH_2)_{12}CH_3$], 49.5 [$CH_2CHN^+(CH_3)_3$], 49.7 [$N^+(CH_3)_3$], 50.3 [$CH_2Ph$], 129.9 (C-5, -6, -8, -9, -14, -15, -17, -18, -23, -24, -26, -27, -32, -33, -35, and -36), 137.0 (C-4, -7, -13, -16, -22, -25, -31, and -34), 167.0 [CH_2CHCON], and 169.4 [CH_2CON]. Anal. Calcd for $C_{172}H_{312}Cl_4N_{12}O_8 \cdot 4H_2O$: C, 71.47; H, 11.15; N, 5.82. Found: C, 71.21; H, 10.75; N, 5.63.

***N*,*N*′,*N*″,*N*‴-Tetrakis[3-(benzyloxycarbonyl)-2-[(*tert*-butoxycarbonyl)amino]propanoyl]-2,11,20,29-tetraaza[3.3.3.3]paracyclophane (9).** Dicyclohexylcarbodiimide (3.31 g, 16 mmol) was added to a solution of N^{α}-(*tert*-butoxycarbonyl)-L-aspartic acid β-benzyl ester (**3**) (4.71 g, 15 mmol) in dry dichloromethane (25 mL) at 0 °C, and the mixture was allowed to stand at the same temperature while being stirred for 50 min. Compound **4** (868 mg, 1.8 mmol) in dry dichloromethane (20 mL) was added to the mixture, and the resulting mixture was stirred for 4 h at 0 °C and for additional 18 h at room temperature. Precipitates that formed (*N*,*N*′-dicyclohexylurea) were removed by filtration, the solvent was eliminated under reduced pressure, and the residue was dissolved in ethyl acetate (70 mL). The solution was then allowed to stand overnight at 5 °C, precipitates were removed by filtration, and the solvent was evaporated off under reduced pressure. The crude product was purified by gel filtration chromatography on columns of Sephadex LH-20 and Toyopearl HW-40F, in this sequence, with methanol–chloroform (1:1 v/v) as eluant. Evaporation of the product fraction under reduced pressure gave a white solid (2.57 g, 84%): mp 92.0–93.1 °C; R_f (Wako Silica Gel 70FM; ethyl acetate) 0.86; IR (KBr disc) 2920 and 2860 (CH), and 1740, 1710, and 1650 (C=O) cm^{-1}; NMR (400 MHz, $CDCl_3$) δ_H 1.36 [36 H, s, $(CH_3)_3CO$], 2.79 [8 H, bd, $COCH_2CH$], 4.33–4.62 [16 H, m, CH_2Ph], 5.12 [8 H, bs, OCH_2Ph], 5.14 [8 H, m, CHN*H*CO and C*H*NHCO], 6.85 [16 H, m, CH_2ArHCH_2], and 7.26 [20 H, m, OCH_2ArH]. Anal. Calcd for $C_{96}H_{112}N_8O_{20} \cdot {}^1/_2H_2O$: C, 67.55; H, 6.67; N, 6.56. Found: C, 67.48; H, 6.70; N, 6.58.

***N*,*N*′,*N*″,*N*‴-Tetrakis[2-[(*tert*-butoxycarbonyl)amino]-3-carboxypropanoyl]-2,11,20,29-tetraaza[3.3.3.3]paracyclophane (10).** Palladium black (10% Pd, 1.0 g) and acetic acid (0.3 mL) were added to compound **9** (1.0 g, 0.59 mmol) in tetrahydrofuran (30 mL), and hydrogen gas was introduced into the mixture at room temperature for 25 h along with stirring. The catalyst was removed by filtration, and the solvent was eliminated under reduced pressure to give a white solid (751 mg, 95%): mp 269.4–270.4 °C dec; R_f (Wako Silica Gel 70FM; methanol) 0.46; IR (KBr disc) 2920 and 2860 (CH), and 1750, 1710, and 1650 (C=O) cm^{-1}; NMR (60 MHz, $CDCl_3$) δ_H 1.35 [36 H, s, $(CH_3)_3CO$], 2.80 [8 H, m, $COCH_2CH$], 4.1–4.6 [16 H, bs, CH_2Ph], 4.9–5.2 [8 H, m, NHC*H*CO and N*H*CHCO], and 6.7–7.2 [16 H, m, ArH]. Anal. Calcd for

$C_{68}H_{88}N_8O_{20}\cdot 2H_2O$: C, 59.46; H, 6.75; N, 8.16. Found: C, 59.32; H, 6.72; N, 8.12.

N,N',N'',N'''-Tetrakis[2-[(*tert*-butoxycarbonyl)amino]-3-(N,N-ditetradecylcarbamoyl)propanoyl]-2,11,20,29-tetraaza[3.3.3.3]paracyclophane (11). Dicyclohexylcarbodiimide (204 mg, 0.99 mmol) was added to a solution of compound **10** (300 mg, 0.22 mmol), ditetradecylamine (736 mg, 1.80 mmol), and 1-oxybenzotriazole (182 mg, 1.35 mmol) in dry tetrahydrofuran (35 mL) at 0 °C, and the resulting mixture was stirred for 2 h at 0 °C and for additional 17 h at room temperature. Precipitates that formed (N,N'-dicyclohexylurea) were removed by filtration, the solvent was eliminated under reduced pressure, and the residue was dissolved in ethyl acetate (50 mL). The solution was then allowed to stand for 90 min at 5 °C, precipitates were removed by filtration, and the solvent was evaporated off under reduced pressure. The crude product was purified by gel filtration chromatography on columns of Sephadex LH-20 and Toyopearl HW-40F, in this sequence, with methanol–chloroform (1:1 v/v) as eluant. Evaporation of the product fraction under reduced pressure gave a colorless glassy solid (560 mg, 86%): IR (KBr disc) 2920 and 2860 (CH), and 1710 and 1640 (C=O) cm^{-1}; NMR (400 MHz, $CDCl_3$) δ_H 0.86 [24 H, J 7.0 Hz, t, $(CH_2)_{13}CH_3$], 1.26 [192 H, m, $CH_2(CH_2)_{12}CH_3$], 1.33 [36 H, s, $(CH_3)_3CO$], 2.83 [8 H, m, $COCH_2CH$], 3.20 [16 H, m, CH_2-$(CH_2)_{12}CH_3$], 4.30 [16 H, m, CH_2Ph], 5.1–5.5 [8 H, m, NHCHCO and CONHCH], and 6.85 [16 H, m, ArH]. Anal. Calcd for $C_{180}H_{316}N_{12}O_{16}\cdot{}^1/_2H_2O$: C, 74.20; H, 10.97; N, 5.77. Found: C, 74.10; H, 10.95; N, 5.63.

N,N',N'',N'''-Tetrakis[2-amino-3-(N,N-ditetradecylcarbamoyl)propanoyl]-2,11,20,29-tetraaza[3.3.3.3]paracyclophane (12). Trifluoroacetic acid (18 mL) was added to a solution of compound **11** (500 mg, 0.17 mmol) in dry dichloromethane (50 mL), and the mixture was stirred for 2 h at room temperature. After the solvent was evaporated off under reduced pressure, the crude product was purified by gel filtration chromatography on a column of Sephadex LH-20 with methanol as eluant. Evaporation of the solvent under reduced pressure gave a pale yellow glassy solid as the trifluoroacetic acid salt (480 mg, 94%): IR (KBr disc) 2920 and 2860 (CH), and 1720 and 1650 (C=O) cm^{-1}; NMR (60 MHz, $CDCl_3$) δ_H 0.88 [24 H, t, $(CH_2)_{13}CH_3$], 1.25 [192 H, m, CH_2-$(CH_2)_{12}CH_3$], 2.70 [8 H, m, $COCH_2CH$], 3.30 [16 H, m, CH_2-$(CH_2)_{12}CH_3$], 4.39 [20 H, m, CH_2Ph and $COCH_2CH$], and 6.77 [16 H, m, ArH]. Anal. Calcd for $C_{160}H_{284}N_{12}O_8\cdot 4(CF_3CO_2H)$: C, 68.17; H, 9.81; N, 5.68. Found: C, 68.19; H, 10.04; N, 5.75.

N,N',N'',N'''-Tetrakis[3-(N,N-ditetradecylcarbamoyl)-2-[(trimethylammonio)acetamido]propanoyl]-2,11,20,29-tetraaza[3.3.3.3]paracyclophane Tetrabromide (2). Triethylamine (99 mg, 1.7 mmol) and the trifluoroacetic acid salt of **12** (246 mg, 8.3×10^{-5} mol) were dissolved in dry dichloromethane (5 mL), and the solution was cooled to 0 °C. Bromoacetyl chloride (108 mg, 0.69 mmol) in dry dichloromethane (5 mL) was added dropwise to the solution at 0 °C with stirring, and the mixture was stirred for 2 h at 0 °C and for additional 14 h at room temperature. The resulting mixture was evaporated to dryness under reduced pressure. The residue was dissolved in dichloromethane (30 mL) and washed with 4% aqueous sodium hydrogen carbonate (25 mL × 1), 4% aqueous citric acid (25 mL × 1), and saturated aqueous sodium chloride (25 mL × 1) in this sequence. After being dried (Na_2SO_4), the solution was evaporated to dryness under reduced pressure, and the residue was dissolved in tetrahydrofuran (30 mL). Dry trimethylamine gas was introduced into this solution for 2.5 h at room temperature, and the solution was stirred at the same temperature for 48 h. The solvent was evaporated off under reduced pressure, and the crude product was purified by gel filtration chromatography on a column of Sephadex LH-20 with methanol as eluant. Evaporation of the solvent under reduced pressure gave a pale brown solid (170 mg, 63.5%): mp 165–167 °C; IR (KBr disc) 2920 and 2860 (CH), and 1690 and 1650 (C=O) cm^{-1}; NMR (400 MHz, $CDCl_3$) δ_H 0.87 [24 H, t, J 7.0 H, $(CH_2)_{13}CH_3$], 1.26 [192 H, m, $CH_2(CH_2)_{12}CH_3$], 2.70 [8 H, bd, $COCH_2CH$], 3.20–3.50 [16 H, m, $CH_2(CH_2)_{12}CH_3$], 3.35 [36 H, s, $N^+(CH_3)_3$], 4.40 [8 H, m, $COCH_2N^+(CH_3)_3$], 4.27–4.80 [16 H, m, CH_2Ph], 5.32 [8 H, m, CONHCH and CONHCH], and 6.73–6.90 [16 H, bd, ArH]; δ_C (100 MHz, CD_3OD) 14.8 [$(CH_2)_{13}CH_3$], 24.0 [$(CH_2)_{12}CH_2CH_3$], 28.3 [$(CH_2)_2CH_2(CH_2)_{10}CH_3$], 28.5 [$COCH_2CH$], 29.2 [$(CH_2)_{10}CH_2(CH_2)_2CH_3$], 30.8 [$(CH_2)_3(CH_2)_7(CH_2)_3CH_3$], 3.14 [$(CH_2)_{11}CH_2CH_2CH_3$], 33.4 [$CH_2CH_2(CH_2)_{11}CH_3$], 49.1 [$NCH_2(CH_2)_{12}CH_3$], 49.9 [$CH_2CHNH$], 50.1 [$N^+(CH_3)_3$], 50.6 [$CH_2Ph$], 55.3 [$COCH_2N^+(CH_3)_3$], 129.2 (C-5, -6, -8, -9, -14, -15, -17, -18, -23, -24, -26, -27, -32, -33, -35, and -36), 137.5 (C-4, -7, -13, -16, -22, -25, -31, and -34), 164.3 [$COCH_2N^+$-$(CH_3)_3$], and 171.3 [CH_2CON and CH_2CHCON]. Anal. Calcd for $C_{180}H_{324}Br_4N_{16}O_{12}\cdot 2H_2O$: C, 66.31; H, 10.14; N, 6.87. Found: C, 66.48; H, 9.88; N, 6.69.

General Measurements. Melting points were measured with a Yanaco MP-500D apparatus (hot-plate type). Elemental analyses were performed at the Microanalysis Center of Kyushu University. IR spectra were recorded on a JASCO IR-810 grating, or a JEOL JIR-AQS20M FT-IR spectrophotometer, a cell of 0.025-mm path length with CaF_2 window being used for solution samples. ^1H and ^{13}C NMR spectra were taken on a Hitachi R-24B spectrometer (60 MHz for ^1H) and a JEOL JNM-GX400 spectrometer (400 and 100 MHz for ^1H and ^{13}C, respectively). Mass spectral measurements were carried out with a JEOL JMS-10SG-2 spectrometer. A Beckman Φ71 pH meter equipped with a Beckman 39505 combined electrode was used for pH measurements after calibration with a combination of appropriate aqueous standard buffers. Surface tension measurements were performed at room temperature with a Shimadzu ST-1 surface tensometer assembled by the Wilhelmy principle, while dynamic light-scattering measurements were performed with a Photal (Otsuka Electronics) dynamic light scattering spectrophotometer DLS-700 (HeNe laser 632.8 nm) equipped with a NEC PC-9801 RA personal computer. A Daini Seikosha SSC-560U calorimeter was used for differential scanning calorimetry. Negatively stained electron micrographs were taken on a JEOL JEM-200CX electron microscope installed at the Research Laboratory for High Voltage Electron Microscopy of Kyushu University, in a manner as described previously.[17] Circular dichroism spectra were run on a JASCO J-500C spectropolarimeter. Fluorescence spectra were recorded on a Hitachi 650-40 fluorescence spectrophotometer, while fluorescence polarization data were measured with a Union Giken FS-501A spectrophotometer equipped with a Sord M200 Mark II microcomputer. Fluorescence lifetimes were recorded on a Horiba NAES-1100 time-resolved spectrofluorometer.

Results and Discussion

Design and Syntheses of Octopus Cyclophanes. In the initial stage of our current studies on molecular recognition by octopus cyclophanes, we have prepared so-called octopus-like hosts by introduction of four hydrophobic chains into a tetraaza[3.3.3.3]paracyclophane skeleton at its nitrogen atoms to secure a deeper hydrophobic cavity,[8,10] since it has been known that an internal cavity provided by this macrocyclic skeleton acts as an effective recognition site toward various hydrophobic guest molecules.[18,19] In aqueous media, hydrophobic guests are effectively incorporated into these hosts primarily through hydrophobic interactions, and the substituted hydrocarbon chains assist in enhancing the binding ability. On this ground, we have then prepared a real octopus cyclophane bearing eight hydrocarbon branches by employing the same macrocyclic skeleton.[9,11] An α-amino acid residue, L-lysine, was used as the molecular component connecting a double-chain segment with the macrocyclic ring and attaching an ionic group which discriminates between guests on the basis of electrostatic effect and confers water solubility on the resulting host.

We have now designed and prepared new octopus hosts bearing L-aspartate residues, **1** and **2**. Both hosts are constituted with the same molecular components, but the connecting modes of L-aspartate moieties are different from each other; β- and α-carboxylato groups of the amino acid residue are connected with the macrocyclic ring and each double-chain segment, respectively, for formation of **1**, whereas the roles of these carboxylate groups are interchanged for **2**. In both host molecules, two C–N bonds having some double-bond character and three C–C single bonds are interposed between the macrocyclic skeleton and each double-chain segment, and the chiral carbon atom is placed in the middle part of the connector unit. Thus, the present octopus cyclophanes seem to possess relatively rigid character at the connector portions (vide infra).

Aggregation Behavior of Octopus Cyclophanes. Prior to study on molecular recognition by the octopus cyclophanes, we examined their aggregation behavior in aqueous media at 21.5 ± 1 °C by means of dynamic light scattering (dls) measurements. When a 1.0 mM aqueous solution of **1** was injected into pure water, the

(17) Murakami, Y.; Nakano, A.; Yoshimatsu, A.; Uchitomi, K.; Matsuda, Y. *J. Am. Chem. Soc.* **1984**, *106*, 3613–3623.

(18) Urushigawa, Y.; Inazu, T.; Yoshino, T. *Bull. Chem. Soc. Jpn.* **1971**, *44*, 2546–2547.

(19) (a) Tabushi, I.; Kuroda, Y.; Kimura, Y. *Tetrahedron Lett.* **1976**, 3327–3330. (b) Tabushi, I.; Kimura, Y.; Yamamura, K. *J. Am. Chem. Soc.* **1978**, *100*, 1304–1306. (c) Tabushi, I.; Kimura, Y.; Yamamura, K. *J. Am. Chem. Soc.* **1981**, *103*, 6486–6492.

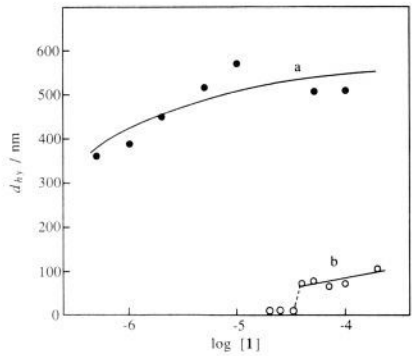

Figure 1. Correlations of hydrodynamic diameter (d_{hy}) of aggregates with concentration of octopus cyclophane **1** in aqueous media at 21.5 ± 1 °C when aqueous (a) and ethanolic (b) stock solutions of **1** (1.0 mM) were injected into water; a final ethanol content for each solution of b was maintained at 1% (v/v).

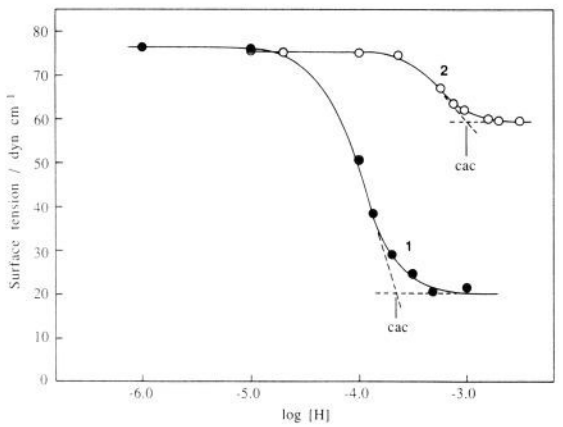

Figure 2. Correlations of surface tension with host concentration [H] (hosts **1** and **2**) in aqueous HEPES buffer (0.01 M, pH 8.0, μ 0.10 with KCl) at room temperature (10 °C).

cyclophane formed relatively large aggregates with hydrodynamic diameters (d_{hy}) of 350–600 nm over a wide concentration range, and the critical aggregate concentration (cac) was not detected in a concentration range above 5.0×10^{-7} M (Figure 1a). Even when a small amount of ethanol [1.0% (v/v)] was added to each aqueous solution, the d_{hy} values were little changed. On the other hand, smaller d_{hy} values (70–100 nm) were obtained by using a 1.0 mM ethanolic solution of **1** in place of the corresponding aqueous stock solution (Figure 1b); the final ethanol content was maintained at 1% (v/v). Since the present dls instrument is capable of detecting aggregates of d_{hy} as low as 3 nm, aggregation of the octopus cyclophane does not occur in the concentration range lower than the detectable limit. Thus, the cac value was evaluated to be 4.0×10^{-5} M under such conditions. The d_{hy} values observed under the above mentioned conditions remained the same for several days, no matter which stock solution was used. This indicates that dissociation of the molecular aggregates into the monomeric species is largely inhibited in aqueous media, presumably due to strong hydrophobic character of the present octopus cyclophane. Analogous aggregation behavior was observed for the other octopus cyclophane (**2**): the d_{hy} value in pure water is in a range of 534–560 nm when a 1.0 mM aqueous stock solution was injected; the cac value in water containing 1.0% (v/v) ethanol is 1.0×10^{-5} M when a 1.0 mM ethanolic solution was injected, and the d_{hy} value above the cac is in a range of 198–242 nm.

We also examined the aggregation behavior of the octopus cyclophanes by means of surface tension measurements (Figure 2). The surface tension (γ) for **1** decreased gradually with an increase in the host concentration, and the cac value was determined to be 2.5×10^{-4} M. The γ value above the cac is 20 dyn cm^{-1}. On the other hand, the cac value for **2** is somewhat larger (1.1×10^{-3} M) and the γ value above the cac is 60 dyn cm^{-1}.

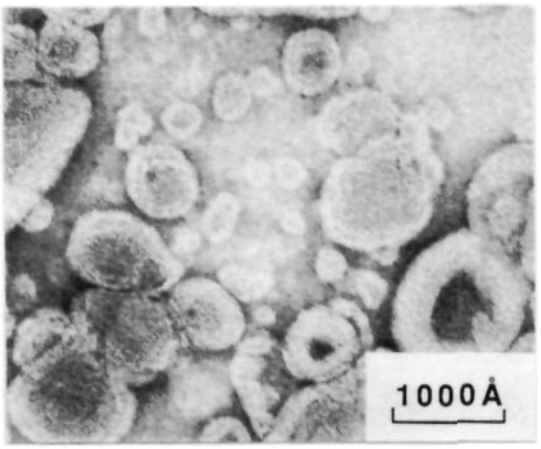

Figure 3. Electron micrograph for aqueous dispersion of **1** (5.0 mM), as negatively stained with uranyl acetate.

Thus, molecular arrangement in a monolayer assembly formed at the air–water interface is very sensitive to molecular architecture in the connector portions of the octopus cyclophane. The cac values obtained from the surface tension measurements disagree with those from the dls measurements. This discrepancy may come from specific aggregation behavior of the octopus cyclophanes at the air–water interface, perhaps quite different from that in the bulk aqueous phase. Similar inconsistency between cac values measured by surface tension and dls methods has been noted for an anionic calix[6]arene derivative bearing six long hydrocarbon chains.[20]

Formation of multiwalled bilayer vesicles in a dimater range of 100–500 nm was observed for aqueous dispersions of **1** (5 mM) by negative-staining electron microscopy (Figure 3). We have previously clarified that synthetic peptide lipids with a general molecular formula of $XC_m(AA)2C_n$, each of which has an amino

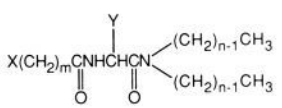

X : polar head group

Y : amino acid side chain

$XC_m(AA)2C_n$

acid residue interposed between a hydrophobic double-chain segment and a polar head moiety, form morphologically stable bilayer membranes in aqueous media.[17,21] In general, a multiwalled bilayer membrane is formed in the dispersion state and transformed into single-walled vesicles upon sonication; the latter vesicles remain without morphological changes for over a month. The characteristic morphological stability of single-walled vesicles formed with the peptide lipids are attributable to formation of hydrogen-belt domains in the aggregates. The present octopus cyclophanes are regarded as tetramers of the peptide lipids, since the four amphiphilic components are assembled together by their linkages to a tetraaza[3.3.3.3]paracyclophane ring via amino acid residues. It needs to be noted, however, that the aggregate morphology of **1** observed in the dispersion state was not subject to any significant change upon sonication by a probe-type sonicator at 30-W power for 1 min, suggesting that less favorable molecular packing caused by the macrocyclic skeleton in the aggregate does not allow the formation of single-walled vesicles. The absence of phase transition from gel to liquid crystalline state for the

(20) Shinkai, S.; Mori, S.; Koreishi, H.; Tsubaki, T.; Manabe, O. *J. Am. Chem. Soc.* **1986**, *108*, 2409–2416.

(21) Murakami, Y.; Kikuchi, J.; Nakano, A. *J. Syn. Org. Chem., Jpn.* **1987**, *45*, 640–653 and references cited therein.

Table I. Formation Constants (K) and Free Energies of Complexation (ΔG) for Host-Guest Complexes of Octopus Cyclophanes with ANS in Aqueous Media[a]

entry	host	host stock solution (1.0 mM)	medium[b]	T, °C	K, M^{-1}	$-\Delta G$, kcal mol^{-1}
1	**1**	H_2O	HEPES	20.0	7.60×10^5	7.89
2	**1**	H_2O	HEPES	30.0	5.30×10^5	7.94
3	**1**	H_2O	HEPES	40.0	4.00×10^5	8.04
4	**1**	H_2O	HEPES	50.0	3.00×10^5	8.11
5	**1**	H_2O	HEPES-0.25% (v/v) EtOH	30.0	5.20×10^5	7.92
6	**1**	H_2O	HEPES-20% (v/v) EtOH	30.0	1.38×10^5	7.13
7	**1**	H_2O	H_2O-20% (v/v) MeOH	30.0	9.78×10^4	6.92
8	**2**	H_2O	HEPES	30.0	7.90×10^5	8.18
9	**2**	H_2O	HEPES-0.25% (v/v) EtOH	30.0	7.51×10^5	8.14
10	**2**	EtOH	HEPES-0.25% (v/v) EtOH	30.0	1.41×10^5	7.13
11	**2**	H_2O	H_2O-20% (v/v) MeOH	30.0	4.20×10^5	7.79
12	**8**	EtOH	MES-0.25% (v/v) EtOH	30.0	3.86×10^5	7.75

[a] Concentrations: ANS, 2.5×10^{-7} M; hosts, 2.5×10^{-7} - 1.4×10^{-5} M. [b] Buffer compositions: 0.01 M, μ 0.10 with KCl; HEPES [*N*-(2-hydroxyethyl)piperazine-*N*'-2-ethanesulfonate] and MES [2-(*N*-morpholino)ethanesulfonate] for pH 8.0 and 5.0, respectively.

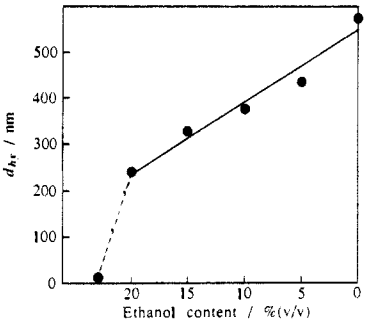

Figure 4. Correlation of hydrodynamic diameter (d_{hy}) of aggregates with ethanol content in aqueous media at 21.5 ± 1 °C for octopus cyclophane **1** (7.0×10^{-6} M) when its aqueous stock solution (1.0 mM) was injected into media.

dispersion sample of **1** in a temperature range of 0–70 °C, as measured by differential scanning calorimetry, evidences much looser molecular packing; typical bilayer aggregates formed with the peptide lipids having comparable double-chain length (n = 14 in $XC_m(AA)2C_n$) show a phase transition at 2 ± 1 °C in the dispersion state.[21]

Figure 4 shows a correlation of the d_{hy} value for **1** with an ethanol content in aqueous media. In this case, an aqueous stock solution (1.0 mM) was injected into aqueous media containing an appropriate volume of ethanol, and the concentration of **1** was maintained at 7.0×10^{-6} M. The d_{hy} value decreases with an increase in the ethanol content, and **1** exists as the monomeric species above 25% (v/v) of ethanol content. The d_{hy} values remained the same for at least one day. Thus, the size of the molecular aggregate seems to be set at the moment of injection of the stock solution.

Influence of Aggregation in Guest-Binding Behavior. In an aqueous HEPES (*N*-(2-hydroxyethyl)piperazine-*N*'-2-ethanesulfonate) buffer (0.01 M, pH 8.0, and μ 0.10 with KCl) containing 20% (v/v) ethanol, the cac value was determined to be 6.0×10^{-6} M by the dls measurements for octopus cyclophane **1** when its aqueous stock solution (1.0 mM) was injected into the buffer solution. In this medium, host–guest complexation behavior between **1** and ANS was examined by changing the host concentration in the range of 2.0×10^{-6} to 1.4×10^{-5} M at a constant guest concentration (2.5×10^{-7} M) and monitoring the fluorescence spectrum of the guest. As shown in Figure 5, the fluorescence intensity originating from ANS increased upon addition of **1**, showing simple saturation behavior, and a Benesi–Hildebrand plot[11,22] based on the 1:1 host–guest complexation was found to be linear (r = 0.999) regardless of the concentration range, above or below the cac. The result clearly indicates that the incorporation of the guest into the host cavity in 1:1 stoichiometry is not disturbed even under conditions in which the host undergoes aggregation.

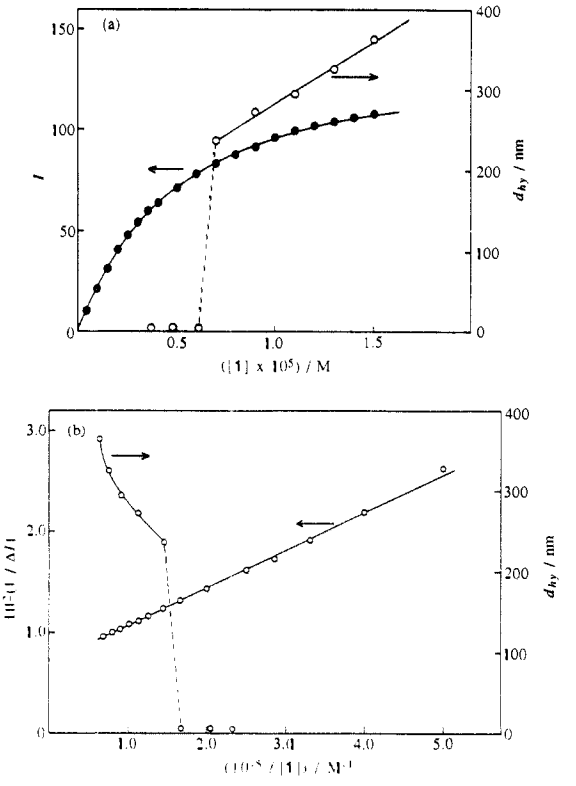

Figure 5. (a) Correlations of fluorescence intensity (I) originating from ANS (2.5×10^{-7} M) and hydrodynamic diameter (d_{hy}) of cyclophane aggregates with concentration of octopus cyclophane **1** when an aqueous stock solution of **1** (1.0 mM) was injected into aqueous HEPES buffer (0.01 M, pH 8.0, μ 0.10 with KCl) containing 20% (v/v) ethanol. (b) Benesi–Hildebrand plot. Excitation and emission wavelengths for fluorescence intensity measurements (also for Figures 8 and 10) are 375 and 468 nm, respectively.

Formation constants for the 1:1 host–guest complexes of the octopus cyclophanes (**1**, **2**, and **8**) and ANS in aqueous media are listed in Table I. All the octopus cyclophanes strongly bind an ANS molecule with binding constants in the 10^5 M^{-1} range in aqueous buffers (entries 1–4, 8, and 12 in Table I). When an aqueous stock solution of each octopus cyclophane was injected into an aqueous buffer containing ANS, the presence of a small amount of ethanol [0.25% (v/v)] little affected the binding constant (entries 5 and 9 in Table I), but the value decreased apparently with an increase in ethanol content owing to a solvent effect that weakens the hydrophobic interaction between the host and the guest (entries 6, 7, and 11 in Table I). On the other hand, the binding constant was lowered 5.4-fold when ethanol was used as a medium for the stock solution in place of water, even though

(22) Benesi, H. A.; Hildebrand, J. H. *J. Am. Chem. Soc.* **1949**, *71*, 2703–2707.

Table II. ^{1}H NMR Signal Shifts for ANS as Induced by Octopus Cyclophanes in D_2O–CD_3OD (80:20 v/v) at 30.0°C[a]

atom	δ (ANS)	δ (1 + ANS)	Δδ(1)	CIS(1)	δ (2 + ANS)	Δδ(2)	CIS(2)
2-H	8.35	8.35	−0.00	−0.00	8.40	+0.05	+0.06
3-H	7.58	7.39	−0.18	−0.22	7.37	−0.21	−0.25
4-H	8.12	7.74	−0.38	−0.45	7.83	−0.29	−0.35
5-H	7.71	7.47	−0.24	−0.29	7.43	−0.28	−0.34
6-H	7.56	7.29	−0.25	−0.35	7.28	−0.26	−0.31
7-H	7.68	7.56	−0.12	−0.14	7.58	−0.10	−0.12
2′-H	7.16	7.14	−0.02	−0.02	7.18	+0.02	+0.02
3′-H	7.33	7.20	−0.13	−0.16	7.24	−0.09	−0.11
4′-H	6.95	6.81	−0.14	−0.17	6.85	−0.10	−0.12

[a] Concentrations: ANS, 3.0×10^{-4} M; hosts, 3.0×10^{-4} M. Me_4Si as an external standard. Δδ(host) = δ(host + ANS) − δ(ANS) (ppm). δ(host + ANS) and δ(ANS) refer to chemical shifts (ppm) for ANS in the presence and absence of the host, respectively.

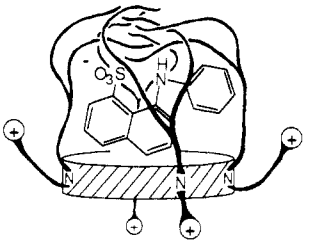

Figure 6. Schematic representation for the host-guest complex of the octopus cyclophane with ANS.

the final ethanol content was very small (compare entries 9 and 10 in Table I). Under the conditions given in Table I, the host–guest complexation reached an equilibrium immediately upon mixing of the host of ANS as monitored by fluorescence intensity originating from the guest molecule. However, unique host–guest complexation behavior was observed when an organic stock solution of the octopus cyclophane, **1** or **2**, was injected into an aqueous buffer containing a guest. Under such conditions, biphasic time courses of the fluorescence parameters were observed. Thus, the guest-binding behavior of the octopus cyclophanes is markedly dependent on the nature of media used for preparation of their stock solutions (vide infra).

^{1}H NMR (400 MHz) signals due to ANS (0.3 mM), as measured in D_2O–CD_3OD (80:20 v/v), showed marked upfield shifts by 0.38, 0.24, and 0.25 ppm for 4-H, 5-H, and 6-H, respectively, and smaller upfield shifts (less than 0.2 ppm) for other protons upon addition of an equimolar amount of **1** (Table II). Since the binding constant under the identical medium conditions as evaluated by fluorescence spectroscopy was 9.8×10^4 M^{-1} (entry 7 in Table I), 80% of the total amount of ANS underwent complexation with **1**. Analogous upfield shifts were observed for ANS signals in the presence of host **2**. The complexation-induced shifts (CIS),[23] the shifts of NMR signals for guest upon 100% complexation, are also listed in Table II. The CIS value is defined by eq 1, where $[G]_0$ and [HG] refer to a total concentration of

$$\mathrm{CIS} = (x - x_f)[G]_0/[HG] \quad (1)$$

a guest and a concentration of a host–guest complex, respectively, while x_f and x stand for NMR chemical shifts originating from a guest in the absence and presence of a host, respectively. The CIS values for the present complexes are not so large in comparison with those for host–guest complexes in which the guest molecule was incorporated into inner macrocyclic cavities of cyclophane hosts.[24-27] Consequently, the ANS molecule is clearly incorporated into the three-dimensional cavity provided intramolecularly by the macrocyclic ring and the eight hydrocarbon chains of the octopus cyclophane as schematically shown in Figure 6.

Table III. Formation Constants (K) and Free Energies of Complexation (ΔG) for Host–Guest Complexes of Octopus Cyclophanes with Various Guests, Microenvironmental Polarity Parameters (E_T^N), and Steady-State Fluorescence Polarization (P) for Guests Incorporated into Cyclophanes in Aqueous HEPES Buffer (0.01 M, pH 8.0, μ 0.10 with KCl) at 30.0 °C

guest	host[a]	K, M^{-1} ($-\Delta G$, kcal mol^{-1})	E_T^N[b] (λ_{ex}, nm; λ_{em}, nm)[c]	P
ANS	**1**	5.3×10^5 (7.94)	0.565 (375; 467)	0.33
ANS	**2**	7.9×10^5 (8.17)	0.565 (375; 468)	0.34
TNS	**1**	1.4×10^6 (8.52)	0.627 (322; 426)	0.32
TNS	**2**	1.3×10^6 (8.48)	0.596 (323; 424)	0.33
α-PNA	**1**	1.0×10^5 (6.93)	0.102 (310; 406)	0.25
α-PNA	**2**	2.1×10^5 (7.38)	0.102 (310; 407)	0.26
β-PNA	**1**	2.3×10^5 (7.43)	0.410 (310; 402)	0.13
β-PNA	**2**	1.4×10^5 (7.14)	0.503 (312; 404)	0.14

[a] H_2O stock solution (1.0 mM). [b] Defined as $E_T^N = [E_T(\text{solvent}) - E_T(\text{TMS})]/[E_T(\text{water}) - E_T(\text{TMS})]$, where E_T refers to a charge transfer energy observed for a specific probe in a solvent indicated in parentheses; E_T^N values assigned to water and tetramethylsilane (TMS) are 1.000 and 0.000 as the most polar and apolar solvents, respectively (ref 28). [c] Excitation and emission maxima are given in parentheses, in this sequence.

The cationic octopus cyclophanes (**1** and **2**) incorporate anionic and nonionic guests, such as ANS, TNS, α-PNA, and β-PNA, through hydrophobic and electrostatic interactions (Table III). On the other hand, the hosts show no capacity for binding guests having the identical charge, such as DASP. As for anionic guests, both of the octopus cyclophanes exhibit binding constants for TNS larger than those for ANS, the former guest having a slender molecular shape relative to the latter. Such molecular discrimination capability of the octopus cyclophanes presumably reflects a more nearly complementary relationship between the β-anilinonaphthalene moiety and the [3.3.3.3]paracyclophane cavity, relative to the corresponding α-isomer, as well as an electrostatic interaction between the host and the guest. Although a CPK molecular model study supports such an interpretation, direct evidence for the conformational differences among these host–guest complexes was not obtained due to lack of appropriate media for ^{1}H NMR measurements of the TNS complexes of the octopus cyclophanes. Even though the molecular shapes of α-PNA and β-PNA are somewhat different from each other; however, significant molecular discrimination does not operate toward these nonionic guests.

The microenvironmental polarities around the incorporated guest molecules were evaluated from their fluorescence maxima in a manner similar to that reported previously.[9,11] The octopus cyclophanes provide relatively apolar microenvironments for the

(23) (a) Schneider, H.-J.; Blatter, T. *Angew. Chem., Int. Ed. Engl.* **1988**, *27*, 1163–1164. (b) Schneider, H.-J.; Rüdiger, K.; Svellana, S.; Ulrich, S. *J. Am. Chem. Soc.* **1988**, *110*, 6442–6448.
(24) Odashima, K.; Itai, A.; Iitaka, Y.; Arata, Y.; Koga, K. *Tetrahedron Lett.* **1980**, *21*, 4347–4350.
(25) Vögtle, F.; Müller, W. M.; Werner, U.; Losensky, H.-W. *Angew. Chem., Int. Ed. Engl.* **1987**, *26*, 901–903.
(26) Diederich, F.; Griebel, D. *J. Am. Chem. Soc.* **1984**, *106*, 8037–8046.
(27) Cowart, M. D.; Sucholeiki, I.; Bukownik, R. R.; Wilcox, C. S. *J. Am. Chem. Soc.* **1988**, *110*, 6204–6210.

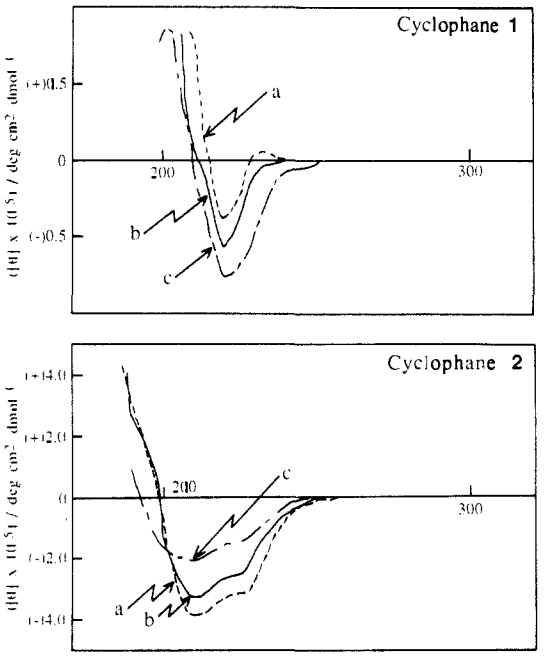

Figure 7. CD spectra of octopus cyclophanes **1** and **2** (1.5×10^{-5} M) in aqueous HEPES buffer (0.01 M, pH 8.0, μ 0.10 with KCl) at 30.0 °C with and without ANS (1.5×10^{-5} M): (a) aqueous stock solutions of the hosts (1.0 mM) were injected in the absence of ANS; (b) aqueous stock solutions of the hosts (1.0 mM) were injected in the presence of ANS; (c) ethanol stock solutions of the hosts (1.0 mM) were injected in the presence and absence of ANS.

various hydrophobic guests (Table III). It must be noted that the fluorescence maxima originating from the incorporated guests are not susceptible to change by the aggregation status of the hosts, monomeric or vesicular. In addition, the E_T^N value[28] (refer to the footnote of Table III) for ANS in each octopus cyclophanes (E_T^N = 0.565; identical with the value for 3-methyl-1-butanol) is smaller than that for ANS bound to the multiwalled bilayer membrane formed with *N,N*-ditetradecyl-N^{α}-[6-(trimethylammonio)hexanoyl]-L-alaninamide bromide [N^+C_5Ala2C_{14}] (E_T^N = 0.700; 0.762 and 0.654 for methanol and ethanol, respectively).[11] Thus, the intramolecular cavities of the octopus cyclophanes are significantly apolar and act as the specific binding sites toward various guest molecules as schematically shown in Figure 6, even in the aggregated state.

Relatively large fluorescence polarization values (P) were obtained for guests, such as ANS, TNS, α-PNA, and β-PNA, incorporated into the octopus cyclophanes (Table III). These values are comparable to those for guests incorporated into other octopus cyclophanes previously prepared, having lysyl residues as the connector units, and the large P values primarily reflect high microscopic viscosity in the hydrophobic cavities of the hosts as discussed previously.[11] The P value is subject to change by the fluorescence lifetime (τ) and the rotational correlation time (θ) of a guest in the light of the following Perrin's equation[29]

$$1/P - 1/3 = (1/P_0 - 1/3)(1 + \tau/\theta) \qquad (2)$$

Here, P_0 refers to the maximal value of P for a probe without any rotational motion. We evaluated P_0, τ, and θ values for ANS incorporated into host **1** by means of time-resolved fluorescence spectroscopy;[30] 0.427, 11.1 ns, and 23.0 ns, respectively. The observed P_0 value for ANS is identical with that obtained from the steady-state fluorescence polarization of ANS in glycerol as

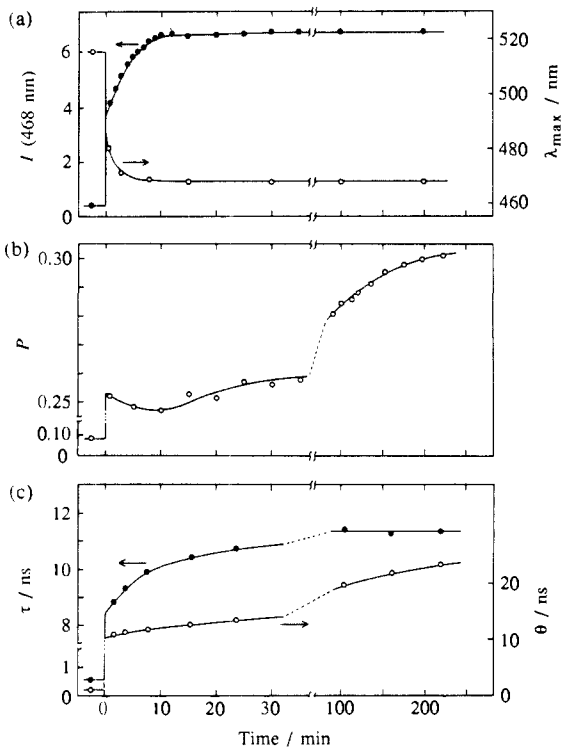

Figure 8. Time courses for changes of fluorescence intensity (I), maximum wavelength (λ_{max}), polarization (P), lifetime (τ), and rotational correlation time (θ) originating from ANS (2.5×10^{-7} M) in aqueous HEPES buffer (0.01 M, pH 8.0, μ 0.10 with KCl) upon addition of an ethanol solution of **1** (2.5×10^{-6} M) at 30.0 °C; final ethanol content, 0.25% (v/v).

reported by Weber and Daniel (P_0 = 0.43).[31] The τ value for ANS bound to the host is large relative to that measured in water (τ = 0.55 ns),[32] and indicates that the guest molecule is placed in a hydrophobic microenvironment well isolated from the bulk aqueous phase. The evaluated θ value is somewhat smaller than that for ANS bound to albumin (θ = 33 ns at 30 °C) but much larger than that for ANS bound to a liposomal membrane formed with lecithin (θ = 3 ns at 30 °C).[33]

Induced-Fit Function of Octopus Cyclophanes. A circular dichroism (CD) study gave us important information as regards the guest-binding behavior of the octopus cyclophanes. Host **1** shows a CD band at 220 nm with a molecular ellipticity ([θ], deg cm^2 dmol^{-1}) of -3.9×10^4 in the HEPES buffer at 30.0 °C by using its aqueous stock solution (Figure 7). Upon addition of an equimolar amount of ANS (1.5×10^{-5} M), the CD spectrum underwent immediate change due to the host–guest complexation to give the [θ] value of -5.6×10^4. A CD spectral change induced by the incorporated ANS molecule was also observed for cyclophane **2** under the identical medium conditions, although the [θ] value at 210 nm decreased upon complex formation from -3.8×10^5 to -3.3×10^5 (Figure 7). Thus, each octopus cyclophane causes conformational changes around the chiral L-aspartate moieties upon complexation with the guest molecule to form a thermodynamically stable host–guest complex.

Thermodynamic parameters for the complexation of **1** with ANS are −5.7 kcal mol^{-1} and 7.2 cal K^{-1} mol^{-1} for ΔH and ΔS, respectively, as evaluated from the data in Table I (entries 1–4). The positive ΔS value comes from effective desolvation of the guest molecule incorporated into the hydrophobic host cavity and partly from conformational change of the host owing to the induced-fit binding of the guest molecule.

Unique biphasic inclusion behavior was observed when an ethanol stock solution of **1** was injected into the aqueous buffer

(28) Reichardt, C. *Solvents and Solvent Effects in Organic Chemistry*; VCH Verlagsgesellschaft: Weinheim, 1988; Chapter 7.
(29) Perrin, M. F. *Ann. Phys.* **1929**, *26*, 169–275.
(30) (a) Spencer, R. D.; Weber, G. *Ann. NY Acad. Sci.* **1969**, *158*, 361–384. (b) Belford, G. G.; Belfold, R. L.; Weber, G. *Proc. Natl. Acad. Sci. U.S.A.* **1972**, *69*, 1392–1393. (c) Lipari, G.; Szabo, A. *Biophys. J.* **1980**, *30*, 489–506. (d) O'Connor, D. V.; Phillips, D. *Time-correlated Single Photon Counting*; Academic Press: London, 1985; Chapter 8.
(31) Weber, G.; Daniel, E. *Biochemistry* **1966**, *5*, 1900–1907.
(32) Yguerabide, J. *Methods Enzymol.* **1972**, *26*, 498–578.
(33) (a) Slavik, J.; Horak, J.; Rihova, L.; Kotyk, A. *J. Membrane Biol.* **1982**, *64*, 175–179. (b) Slavik, J. *Biochim. Biophys. Acta* **1982**, *694*, 1–25.

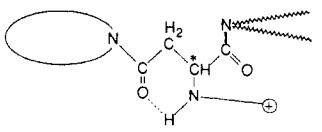

1

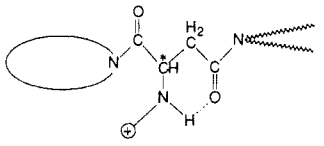

2

Figure 9. Plausible conformational status around the L-aspartate moieties of **1** and **2** in organic media.

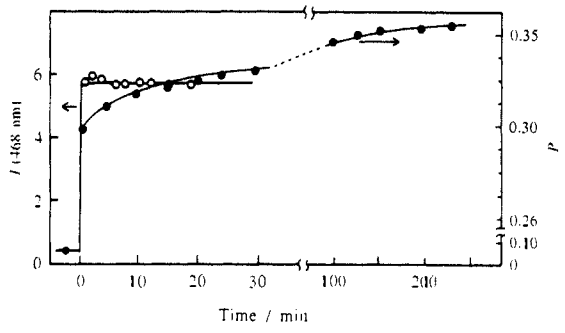

Figure 10. Time courses for changes of fluorescence intensity (I) and polarization (P) originating from ANS (2.5×10^{-7} M) in aqueous HEPES buffer (0.01 M, pH 8.0, μ 0.10 with KCl) upon addition of an ethanol solution of **2** (2.5×10^{-6} M) at 30.0 °C; final ethanol content 0.25% (v/v).

containing ANS in place of an aqueous stock solution under otherwise identical conditions. As shown in Figure 8a, the fluorescence intensity (I) and its maximum (λ_{max}) originating from ANS showed biphasic time courses upon addition of an ethanol solution of **1** into the aqueous buffer solution of ANS. Under the conditions indicated in Figure 8, aggregation of the host molecule does not take place. This behavior is consistent with fast incorporation of the guest molecule into the hydrophobic host cavity followed by slow and long-range conformational changes of the host, as induced by the incorporated guest. At the final stage of such behavior, a highly desolvated microenvironment is apparently provided so that the tight host–guest interaction becomes effective. The apparent rate for the second step of the biphasic complexation was independent of the host concentration, suggesting that this is a unimolecular process operated by the octopus cyclophane. The K value at the final state was evaluated to be 2.0×10^5 M^{-1} from the infinite I values at various host concentrations, comparable to that evaluated for the aqueous stock solution system. The P parameter was also acutely sensitive to the complexation behavior (Figure 8b). The apparently complicated time course was analyzed in terms of the lifetime (τ) and the rotational correlation time (θ) (Figure 8c) on the basis of Perrin's equation (refer to eq 2). The τ and θ values for the ANS molecule showed biphasic time courses in the process of its noncovalent binding to the octopus cyclophane. The analogous biphasic behavior was observed also for the host–guest complexation between **1** and ANS by using other organic stock solutions of the host, prepared with methanol, tetrahydrofuran, and dioxane, and by utilizing other hydrophobic guests, such as TNS, α-PNA, and β-PNA, in place of ANS.

Host **1** showed a CD band at 220 nm with a [θ] value of -7.6×10^4 in ethanol at 30.0 °C. The identical CD spectrum was observed when its ethanol stock solution was injected into the aqueous buffer [Figure 7; the final ethanol content, 0.25% (v/v)], and no spectral change was observed for at least one day at 30.0 °C. Upon addition of an equimolar amount of ANS (0.5×10^{-5} M), the [θ] value remained the same over one day even though the complexation took place. This result indicates that the L-aspartate residues of **1** assume highly restricted conformations in the organic solution and do not undergo conformational changes to any detectable extent even after **1** was injected into the aqueous medium and the guest incorporation took place subsequently. We examined the conformational fixation and stability at the L-aspartate residues in aqueous media after injection of the ethanol stock solution of **1**. Upon addition of ANS (final concentration, 2.5×10^{-7} M) to the aqueous buffer solution containing **1** (2.5×10^{-6} M), which was prepared by injection of an ethanol stock solution (1.0×10^{-3} M) into the aqueous buffer (final ethanol content, 0.25% (v/v)) and incubated at 30.0 °C for 1.5 h, biphasic time courses of the fluorescent parameters similar to those shown in Figure 8 were observed. However, such biphasic behavior became obscured when ANS was added to the above host solution which was incubated at 70.0 °C for 22 h, and the CD spectral intensity originating from the host decreased to half the initial value ([θ] at 220 nm, -3.9×10^4). This observation undoubtedly

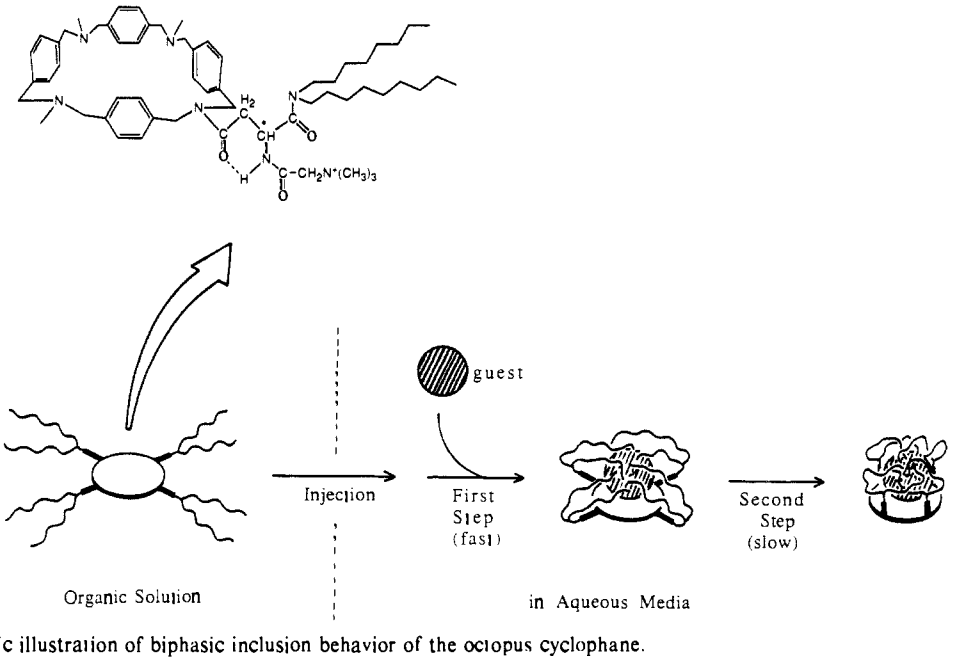

Figure 11. Schematic illustration of biphasic inclusion behavior of the octopus cyclophane.

indicates that the intramolecular hydrogen bonds at the connector portions of the host undergo cleavage at higher temperatures, so that conformational changes take place in a manner as observed by using an aqueous stock solution of the host (vide supra). The stable intramolecular hydrogen bonding (Figure 9), which brings about restricted conformation of the chiral moieties, must be responsible for the biphasic inclusion behavior, observed at ordinary temperatures, as evidenced by FT-IR spectroscopy: C=O stretching bands for the tertiary amides of **1** [1% (w/v)] appeared at 1642 and 1634 cm^{-1} in D_2O and CD_3OD, respectively, suggesting that **1** forms stronger hydrogen bonds in the latter medium.

Octopus cyclophane **2** also exhibited similar biphasic inclusion behavior when its organic stock solutions were injected into aqueous media. As shown in Figure 10, the *P* value for fluorescence from ANS showed a biphasic time course upon addition of an ethanol solution of **2** into the aqueous buffer solution of ANS. However, the biphasic behavior was not reflected in the *I* and λ_{max} parameters; λ_{max} was 468 nm under the medium conditions given in Figure 10. The different responses of the biphasic behavior exhibited by **2** on the fluorescence parameters, as compared with those by **1**, undoubtedly originate from some differences in configuration around the connecter units between the host molecules. The CD spectrum of **2**, observed after its ethanol stock solution was injected into the aqueous buffer, did not undergo any significant change upon complexation with ANS (Figure 7). Since host **2** is able to form stable intramolecular hydrogen bonds as schematically shown in Figure 9, the biphasic behavior presumably comes from such rigid conformation of the L-aspartate residues as pointed out for cyclophane **1**. This conclusion was further evidenced by the following observations: (1) stable intramolecular hydrogen bonds are not formed in **8** due to lack of amide N–H groups as effective hydrogen donors, and **8** did not show detectable biphasic complexation behavior in regards to the time course of fluorescence intensity change under comparable conditions; (2) host **13**, bearing no N–H group, is incapable of forming intramolecular hydrogen bond; when ANS was added to the buffer solution containing **13**, which was injected in advance as an ethanol stock solution and incubated for 60 min at 30 °C, fluorescence intensity of the guest retained the same level without showing biphasic behavior for the comparable period of time. Plausible biphasic guest-binding modes exercised by the present octopus cyclophanes are schematically shown in Figure 11.

Concluding Remarks

The octopus cyclophanes, having L-aspartate residues as connector units interposed between a rigid macrocyclic skeleton and four double hydrocarbon chain segments, exercise two types of guest-binding behavior, depending on the nature of their stock solutions. The octopus cyclophane undergoes aggregation to form large multiwalled bilayer vesicles when its aqueous stock solution is injected into aqueous media. However, the host incorporates various guests through hydrophobic and electrostatic interactions to form 1:1 host–guest complexes regardless of its aggregation status, monomer or vesicle. Significant conformational changes are induced in the host at the chiral L-aspartate residues immediately when a guest molecule is incorporated into the three-dimensional cavity provided by the juxtaposition of the macrocyclic ring and the eight hydrocarbon chains. On the other hand, when an organic stock solution of the octopus cyclophane was injected into an aqueous buffer, its critical aggregate concentration depended on a content of an organic solvent, and the aggregate size was much smaller than that observed by using an aqueous stock solution even at identical concentrations. In the monomeric state of the host, the L-aspartate residues are conformationally fixed due to formation of the strong intramolecular hydrogen bonds, which are already formed in the organic stock solution before its injection into aqueous media. Such restricted conformation is retained even when a guest molecule is incorporated into the host. As a result, biphasic complexation behavior is observed as reflected in various fluorescence parameters, such as fluorescence intensity, maximum, polarization, lifetime, and rotational correlation time, attributable to an included guest. This behavior is consistent with fast incorporation of the guest molecule into the hydrophobic host cavity followed by slow and long-range conformational changes of the host, as induced by the incorporated guest. Such biphasic complexation behavior is acutely sensitive to the molecular architecture at the connector portions of the hosts.

To the best of our knowledge, the present findings can be cited as the first successful example of the induced-fit complexation in artificial host–guest systems from the dynamic viewpoint. We believe that the present results provide a useful guidepost for designing functionalized cyclophane hosts as artificial receptors and enzymes capable of performing induced-fit functions.

Acknowledgment. We are grateful to Dr. Kazunori Sakata of Kyushu Institute of Technology for mass spectroscopic measurements. The present work was supported in part by a Grant-in-Aid for Scientific Research No. 01470097 from the Ministry of Education, Science, and Culture of Japan.

Registry No. **1**, 7536-58-5; **2**, 129215-38-9; **3**, 7536-58-5; **4**, 98001-24-2; **5**, 129194-28-1; **6**, 129194-29-2; **7**, 129194-30-5; **8**, 129194-31-6; **9**, 129215-39-0; **10**, 129194-32-7; **11**, 129194-33-8; **12**, 129194-34-9; **13**, 129194-35-0; ANS, 82-76-8; TNS, 7724-15-4; α-PNA, 90-30-2; ε-PNA, 135-88-6; $[H_3C(CH_2)_{13}]_2NH$, 17361-44-3; $BrCH_2COCl$, 22118-09-8; NMe_3, 75-50-3.